PAPER

Electron impact excitation of bismuth

To cite this article: Aloka Kumar Sahoo and Lalita Sharma 2024 *Phys. Scr.* **99** 095410

Physica Scripta

PAPER

Electron impact excitation of bismuth

Aloka Kumar Sahoo and Lalita Sharma
Department of Physics, Indian Institute of Technology Roorkee, Roorkee-247667, Uttarakhand, India
E-mail: lalita.sharma@ph.iitr.ac.in

RECEIVED
2 July 2024
REVISED
25 July 2024
ACCEPTED FOR PUBLICATION
14 August 2024
PUBLISHED
28 August 2024

Keywords: relativistic distorted wave approximation, cross sections, generalized oscillator strength

Abstract

The present study investigates the electron impact excitation of bismuth from the ground state $6p^3\ ^4S_{3/2}$ to the excited state $6p^27s\ ^4P_{1/2}$. Motivated by the latest measurements by Marinković *et al* [J. Phys. B, 49 23 520 (2016)], relativistic distorted wave calculations are performed to obtain the differential and integrated cross sections for incident electron energies at 10, 20, 40, 60, 80, and 100 eVs. These results are compared with the available experimental data and a good agreement is observed. Our results represent the first theoretical work to provide such a comparison. Additionally, we report the generalized oscillator strengths derived from our calculated differential cross sections.

1. Introduction

Bismuth (Bi), a heavy atom with atomic number 83, provides a testing ground for developing relativistic and many-body methods. It also holds importance in astronomy and astrophysics as Bi is detected in Hg-Mn and χ Lupi stars [1–3]. The theoretical investigation of the electron impact excitation (EIE) of bismuth presents a complex challenge due to open p-shell electrons. In its ground state, Bi has three electrons with electronic configuration [Hg] $6p^3$, represented by the $^4S_{3/2}$ term in the LS coupling scheme. The open-shell structure makes obtaining accurate atomic wavefunctions for the states of Bi challenging because of strong electron correlation effects. Also, in the $T-$ matrix evaluation for EIE of open-shell atoms, angular momentum coupling between different bound states becomes complicated and requires special attention. The difficulty in theoretical calculations is also highlighted in the study of Marinković *et al* [4], who measured the differential cross sections (DCS) for the electron impact excitation of bismuth from the ground state $6p^3\ ^4S_{3/2}$ to the excited state $6p^27s\ ^4P_{1/2}$. The DCS measurements were done over a scattering angle range 2–150 degrees for incident electron energies of 10, 20, 40, 60, 80, 100 eVs. They also reported the generalized oscillator strengths (GOS), integral, momentum transfer and viscosity cross sections at these energies.

Apart from the experimental results of Marinković *et al* [4], only one study is available for EIE of Bi. Williams *et al* [5] reported measurements of DCS for the EIE of $6p^27s\ ^4P_{1/2}$ state from the ground state over the scattering angle range of 0–130 degrees at 40 eV incident electron energy. They also provided integrated cross sections (ICS) for this excitation. On the theoretical side, investigations of the EIE of Bi are limited, focusing primarily on the elastic scattering of electrons. To our knowledge, no theoretical work exists specifically on the EIE of Bi. This gap in theoretical study is emphasized in the work of Marinković *et al* [4]. Therefore, in light of these measurements, we carried out relativistic distorted wave (RDW) calculations for the EIE of bismuth from the ground state $6p^3\ ^4S_{3/2}$ to the excited state $6p^27s\ ^4P_{1/2}$ and reported DCS and ICS.

This paper is organized as follows: section 2 outlines the RDW theory used in our study. Section 3 presents our calculated DCS and ICS results, compared with the experimental data [4, 5]. We also report the GOS. Finally, the conclusion of our work is summarized in section 4.

2. Theory

With the gradual increase in nuclear charge, the spin-orbit interaction dominates over the coulomb interaction between the electrons, and the applicability of the jj-coupling scheme becomes more appropriate. Thus, a

relativistic approach is necessary for studying a heavy element like Bi's atomic properties and interaction with incident electrons. In the present work, we have implemented the relativistic distorted wave approximation, a first-order perturbation method, to study the electron impact excitation of Bi. The RDW approximation is a well-tested theory that exhibits its efficacy across various atomic and ionic systems, especially at intermediate to high electron energies. Our implementation of the RDW method aligns with established practices in prior studies [6–10]. In this method, the transition ($T-$) matrix for electron impact excitation from the initial atomic state $|\alpha_i J_i M_i\rangle$ to final atomic state $|\alpha_f J_f M_f\rangle$ is given by

$$T_{i\to f}^{DW} = \langle \alpha_f J_f M_f,\ \mathcal{E}_b \mu_b | V - U | \alpha_i J_i M_i,\ \mathcal{E}_a \mu_a \rangle. \tag{1}$$

Here, $|\alpha JM,\ \mathcal{E}\mu\rangle$ represents the total wavefunction as the product of bound $|\alpha JM\rangle$ and continuum $|\mathcal{E}\mu\rangle$ states wavefunctions. J, M refer to the total angular momentum quantum number and its associated magnetic quantum numbers to describe the target's state. $\mathcal{E}$ is the projectile electron energy, and μ represents the spin projection of the projectile electron. The subscript i or f represents the atomic bound state in the initial or final state, respectively, and a or b denotes the projectile electron in the initial or final channel. V denotes the interaction potential between the projectile electron and the target atom, and U is the distortion potential experienced by the projectile electron. In the present case, the atomic wavefunctions $|\alpha JM\rangle$ for bismuth are obtained with multiconfiguration Dirac-Hartree–Fock (MCDHF) approach using the GRASP2018 [11] package. A comprehensive theory on the MCDHF approach as implemented in GRASP2018 can be found in the work of Jönsson *et al* [12]. Our calculation procedure for obtaining bismuth's atomic wave function is discussed in the next section 3.1.

The distorted wavefunction of the projectile electron in the incident or scattered channels is written using the Dirac partial wave expansion as,

$$|\mathcal{E}\mu\rangle = \frac{1}{(2\pi)^{3/2}} \sum_{\kappa m} e^{\pm i\Delta_\kappa}\, a_{\kappa m}^{\mu}(\hat{\boldsymbol{k}}) \frac{1}{r} \begin{pmatrix} f_\kappa(r)\chi_{\kappa m} \\ i g_\kappa(r)\chi_{-\kappa m} \end{pmatrix}, \tag{2}$$

$$a_{\kappa m}^{\mu}(\hat{\boldsymbol{k}}) = 4\pi i^l \left[\frac{\mathcal{E}+c^2}{2\mathcal{E}}\right]^{1/2} \sum_{m_l} (l m_l\ 1/2\mu | jm)\ \mathrm{Y}_{lm_l}^{*}(\hat{\boldsymbol{k}}). \tag{3}$$

Here, κ denotes the relativistic quantum number, l represents the corresponding orbital angular momentum quantum number, and m_l is its associated magnetic quantum number. j is the total angular momentum quantum number and m the magnetic quantum number. c represents the speed of light in free space. f_κ and g_κ are the large and small radial components of the projectile electron. These radial components are obtained numerically [13] by solving the following coupled Dirac equations,

$$\left(\frac{\mathrm{d}}{\mathrm{d}r} + \frac{\kappa}{r}\right) f_\kappa(r) - \frac{1}{c}(\mathcal{E} - U + 2c^2) g_\kappa(r) = 0, \tag{4}$$

$$\left(\frac{\mathrm{d}}{\mathrm{d}r} - \frac{\kappa}{r}\right) g_\kappa(r) + \frac{1}{c}(\mathcal{E} - U) f_\kappa(r) = 0. \tag{5}$$

The phase shift Δ_κ of the projectile electron in equation (2) is obtained with the asymptotic boundary conditions,

$$f(r) \overset{r\to\infty}{\to} \frac{1}{k} \sin\left(kr - l\frac{\pi}{2} + \Delta_\kappa\right), \tag{6}$$

$$g(r) \overset{r\to\infty}{\to} \frac{c}{2c^2+\mathcal{E}} \cos\left(kr - l\frac{\pi}{2} + \Delta_\kappa\right). \tag{7}$$

Here, k is the wave number of the projectile electron. These continuum wave functions are generated with our own program, which has been used successfully for several studies in the past [10, 14, 15]. Further, we have considered the distortion potential U as a Dirac-Fock-Slater potential [16, 17] which is written as,

$$U(r) = V^N(r) + \int_0^\infty \frac{\rho(r')}{r_>} r'^2 \mathrm{d}r' - \left(\frac{3}{\pi}\rho(r)\right)^{1/3}, \tag{8}$$

$$\rho(r) = \frac{1}{4\pi r^2} \sum_{j\ \in\ \text{all subshells}} \mathcal{N}_j [P^2_{(n'\kappa')_j}(r') + Q^2_{(n'\kappa')_j}(r')]\mathrm{d}r'. \tag{9}$$

Here, $V^N(r)$ is the nuclear potential considered as the Fermi charge distribution [18]. $r_>$ denotes the maximum between r and r'. ρ represents the electron charge density of the target atom. $P_{(n'\kappa')_j}(r')$ and $Q_{(n'\kappa')_j}(r')$ are the large and small components of the radial part of the j^{th} subshell of the atomic bound state, with principal quantum number n' and relativistic quantum number κ'. $\mathcal{N}_j$ refers to the occupation number of the j^{th} subshell.

Further, it is assumed that the direction of the incident electron is along the z-axis. Using the partial wave expansion of projectile electron from equation (2), the transition matrix (equation (1)) can be rewritten in the following form,

$$T_{i\to f}(M_i,\, M_f,\, \mu_a,\, \mu_b,\, \theta) = \frac{1}{\pi}\left[\frac{(\mathcal{E}_a + c^2)(\mathcal{E}_b + c^2)}{\mathcal{E}_a\mathcal{E}_b}\right]^{1/2} \sum_{\substack{\kappa_a,\kappa_b,\\ m_b,m_{l_b}}} e^{i(\Delta_{\kappa_b}+\Delta_{\kappa_a})} i^{l_a-l_b} \times (l_a 0 \frac{1}{2}\mu_a | j_a \mu_a)(l_b m_{l_b} \frac{1}{2}\mu_b | j_b m_b) \sqrt{\frac{2l_a+1}{4\pi}}\, Y_{l_b m_{l_b}}(\hat{\boldsymbol{k}}) \sum_{J_t,M_t} (J_i M_i j_a \mu_a | J_t M_t) \times (J_f M_f j_b m_b | J_t M_t) \langle (\alpha_f J_f,\, \mathcal{E}_b l_b j_b) J_t || V - U || (\alpha_i J_i,\, \mathcal{E}_a l_a j_a) J_t \rangle. \tag{10}$$

The inherently complex nature of open-shell atoms presents a challenge in properly evaluating the angular momentum coupling coefficients in the reduced matrix elements $\langle (\alpha_f J_f,\, \mathcal{E}_b l_b j_b) J_t || V - U || (\alpha_i J_i,\, \mathcal{E}_a l_a j_a) J_t \rangle$ in equation (10). This complexity could have contributed to the scarcity of theoretical investigations into the EIE of bismuth. To address this challenge, we have adopted the quasi spin formalism for angular momentum theory with second quantization approach and irreducible tensorial sets as proposed by Gaigalas [19]. This methodology provides a robust framework for evaluating the angular momentum coupling coefficients. Details about this approach can be found in the report of Gaigalas [19] and associated references therein. This methodology has successfully demonstrated its efficacy in atomic structure packages like GRASP2018 [11] and Jena atomic calculator (JAC) [20, 21] to compute angular momentum coupling coefficients for systems with an arbitrary number of open-shells. The flexible atomic code [22] also adopts a similar procedure [19] and calculates the collision strengths and integrated cross sections. However, it does not provide the differential cross sections, at least not within the core functionalities of the package.

The convergence of the $T-$ matrix in equation (10) is checked upto 10^{-5} and maximum value of l is taken 250. Since the contribution from the higher partial waves comes primarily at a large radial distance, we considered a larger radial grid spanning up to 200 atomic units in our calculations.

Finally, the DCS can be obtained from the transition matrix as

$$\frac{\mathrm{d}\sigma}{\mathrm{d}\Omega} = \frac{(2\pi)^4}{2(2J_i+1)}\left(\frac{k_b}{k_a}\right) \sum_{M_i,\mu_a,M_f,\mu_b} |T^{DW}_{i\to f}|^2. \tag{11}$$

The integral excitation cross section is obtained by integrating the DCS over the solid angles(Ω). The GOSs can be derived from the DCS as [23]

$$\mathrm{GOS}(K^2,\, \mathcal{E}) = \frac{\Delta E\; k_a}{2\; k_b} K^2 \frac{\mathrm{d}\sigma}{\mathrm{d}\Omega}. \tag{12}$$

Here K^2 is the square of the magnitude of momentum transfer and $\Delta E\,(= E_f - E_i)$ is the minimum excitation energy.

3. Results

3.1. Atomic wavefunction

The first and crucial step in the study of EIE is to obtain reliable atomic wavefunctions for Bi, which are generated using the multiconfiguration Dirac-Hartree–Fock (MCDHF) approach employed in the GRASP2018 package [11]. Our primary objective is to optimize the two levels, viz., ($6p^3\ {}^4S_{3/2}$ and $6p^3 7s\ {}^4P_{1/2}$) of our interest. We have followed the restricted active set approach with the single- and double-excitations from multi-reference set comprising of $\{6p^3, 6p^2 7s\}$. We began the calculation by optimizing the multireference set, followed by the single and double excitation from the valance shells of both multireference configurations to the active set $\{8s,7p,6d,5f\}$. Subsequently, the active set was gradually increased to $\{10s,9p,8d,7f\}$, resulting in 949 configuration state functions (CSF), of which five of the main contributing CSFs for the two levels are,

$$6p^3\ {}^4S_{3/2} = 0.9055\ 6\overline{p}_0^2 6p_{3/2} + 0.3510\ 6\overline{p}_{1/2} 6p_2^2 - 0.1896\ 6p_{3/2}^3 + 0.0683\ (6\overline{p}_{1/2} 6\overline{d}_{3/2})_2 6d_{5/2} + 0.0593\ 6p_{3/2} 6\overline{d}_0^2 \tag{13}$$

$$6p^2 7s\ {}^4P_{1/2} = 0.9694\ 6\overline{p}_0^2 7s_{1/2} - 0.1863\ 6p_0^2 7s_{1/2} + 0.0600\ (6\overline{p}_{1/2} 6p_{3/2})_1 7s_{1/2} + 0.0598\ 6\overline{d}_0^2 7s_{1/2} + 0.0534\ (6\overline{p}_{1/2} 6\overline{d}_{3/2})_1 7p_{3/2} \tag{14}$$

The dominance of a single relativistic CSF indicates a strong jj-coupling nature rather than LS-coupling. However, contributions from other CSFs are essential for a more accurate representation of the energy levels and transition rates between the two levels. From this calculation procedure, the excitation energy and oscillator

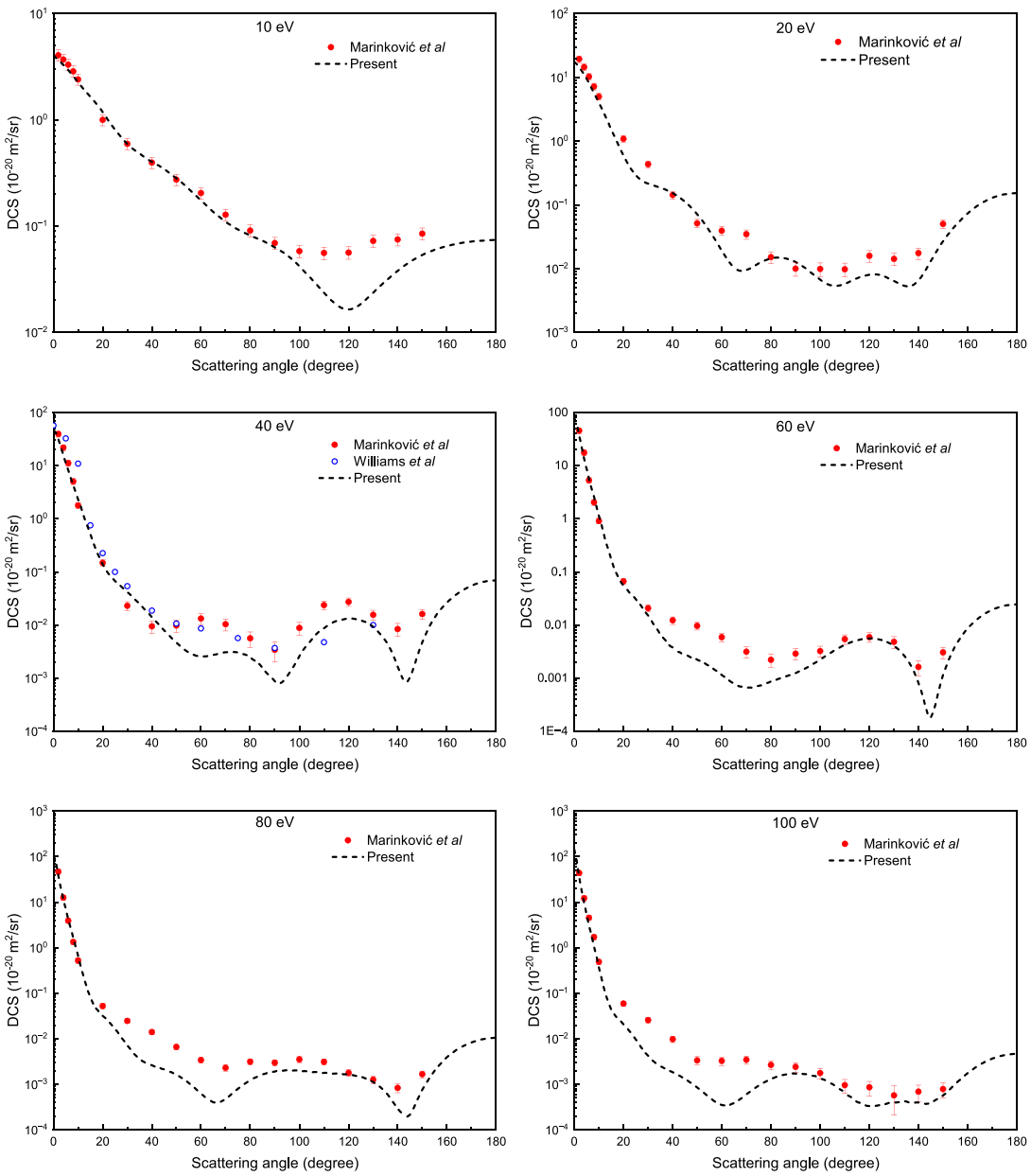

Figure 1. Differential cross sections for electron impact excitation from $6p^3\ ^4S_{3/2}$ to $6p^27s\ ^4P_{1/2}$. Red solid circle: measurements, Marinković *et al* [4]; blue circle: measurements, Williams *et al* [5]; black dashed line: present calculation.

strength for the transition between the levels $6p^3\ ^4S_{3/2}$ and $6p^37s\ ^4P_{1/2}$ are found to be 3.900 eV and 0.122. The ratio of oscillator strength in the Coulomb and Babushkin gauges is 0.902, which shows a good agreement between the two values. Further, our calculated energy and oscillator strength match well with the respective values compiled at the NIST database [24], where energy is listed as 4.040eV [25] and oscillator strength is 0.118 [26].

3.2. Cross sections

We have computed the DCS and ICS for electron impact excitation of bismuth from the ground state $6p^3\ ^4S_{3/2}$ to the excited state $6p^27s\ ^4P_{1/2}$ across an incident electron energy range 10–100 eV. Our calculated DCSs are presented in figure 1 alongside a comparison with the measured cross sections of Marinković *et al* [4] and Williams *et al* [5]. Marinković *et al* [4] utilized an oscillator strength value of 0.146 to normalize their measured differential cross sections (DCSs), referencing this value from the experimental data reported in the CRC [27]. The oscillator strength calculated in the present study is lower than this value. We observed quite good agreement between our calculated DCSs and the experimental data, especially considering the complexity of the target atom, in both forward-scattering and back-scattering angles for all reported energies, except at 10 eV, where our DCS underestimated the back-scattering angles. Nonetheless, the DCSs for 10 eV exhibited excellent

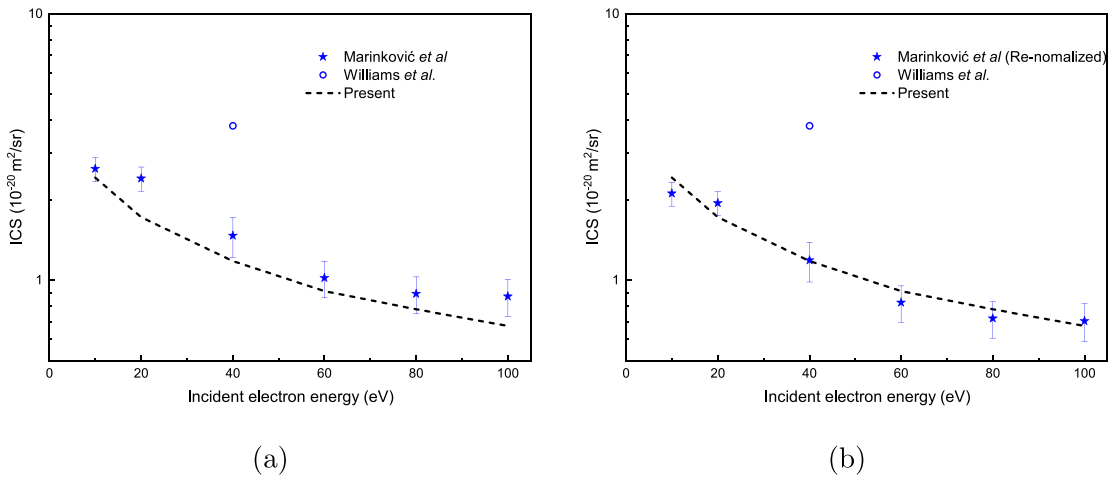

Figure 2. Comparison of the present integrated cross sections for electron impact excitation from $6p^3\ ^4S_{3/2}$ to $6p^27s\ ^4P_{1/2}$ with measurements normalized with oscillator strength values a) 0.146 and b) 0.122. Blue star: measurements, Marinković *et al* [4]; blue circle: measurements, Williams *et al* [5]; black dashed line: present calculation.

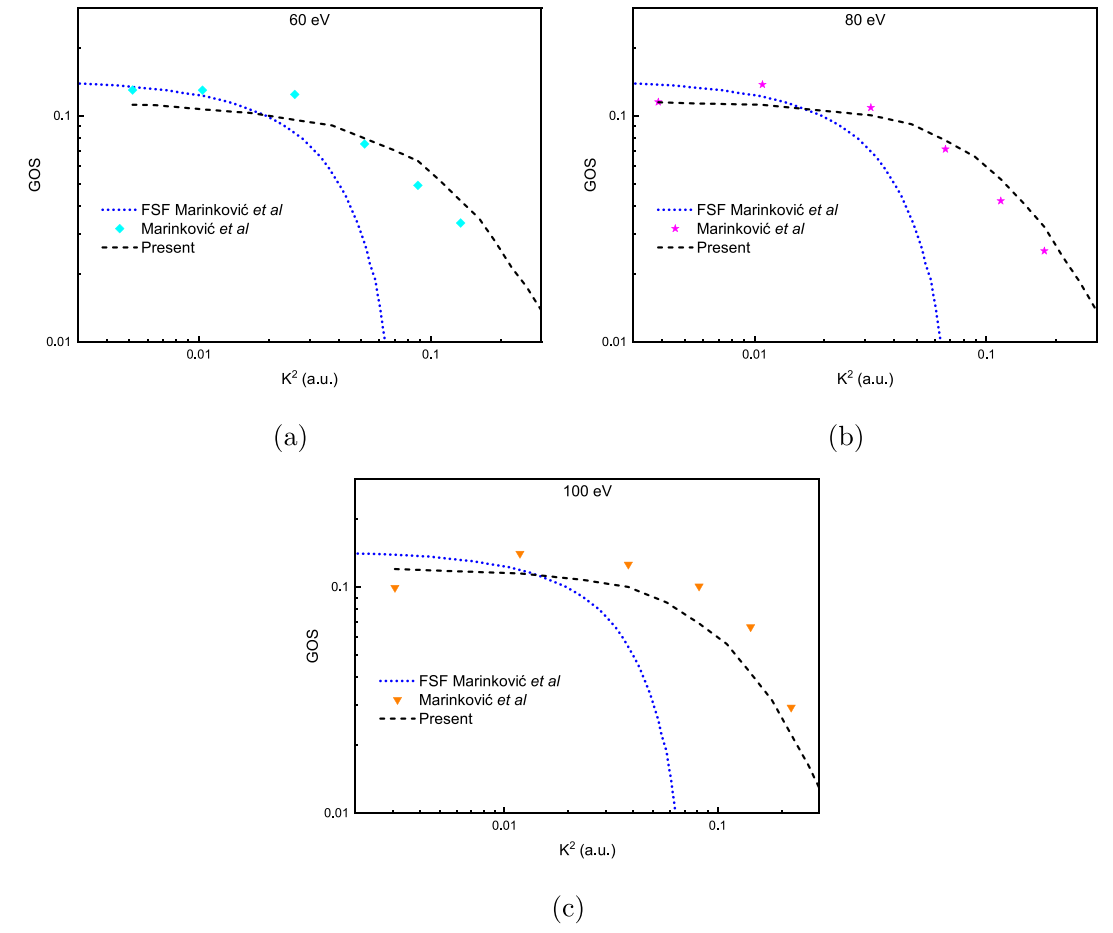

Figure 3. Generalized oscillator strength against the squared momentum transfer (K^2) for electron impact excitation from $6p^3\ ^4S_{3/2}$ to $6p^27s\ ^4P_{1/2}$. Scattered data: Marinković *et al* [4]; black dashed line: present calculation. Blue dotted line: forward scattering function (FSF) Marinković *et al* [4].

agreement up to 100 degrees of scattering angles. At intermediate scattering angles, our calculated DCSs underestimated the measurements for higher incident electron energies within the range of 40–100 eV. However, overall, our obtained DCSs retained the features and shapes reported in the measurements across all electron energies.

The integrated cross sections are reported in figure 2(a) accompanied by a comparison with the reported ICSs by Marinković *et al* [4] in the energy range 10–100eV and the ICS by Williams *et al* [5] at 40 eV. Our calculated ICSs show a reasonable match with the measured ICSs [4] and are mostly within the uncertainty range, except for 20 eV, where it underestimates the measured data. The experimental ICS at 40 eV by Williams *et al* [5] largely overestimates our calculation as well as the results of Marinković *et al* [4]. This discrepancy is well explained by Marinković *et al* [4], where they discussed about the adopted normalization procedure resulting in higher DCSs at the forward scattering angles, consequently increasing the ICS. As discussed in section 3.2, the reported measured cross sections by Marinković *et al* [4] were normalized by oscillator strength of 0.146 which is higher than our calculated oscillator strength of 0.122 and other experimental value 0.118 [26]. Thus, to see the effect of normalization, we re-normalized the measured ICSs with the oscillator strength 0.118, and the comparison is presented in figure 2(b). These re-normalized ICSs show a better agreement with our calculated ICSs. A similar improvement is seen in the DCS values for the forward scattering angles, but this comparison is not shown here for brevity.

The generalized oscillator strengths calculated from the present DCSs are illustrated in figure 3 along with the calculated GOS by Marinković *et al* [4] from their measured DCSs. The GOS obtained for near-zero momentum transfer is ≈ 0.120 at higher incident electron energies, which aligns with our calculated oscillator strength from the atomic wavefunction/structure calculations with the MCDHF approach. Overall, our calculated GOSs exhibit lower magnitude at lower K^2 values compared to that of Marinković *et al* [4]. This discrepancy could be due to the oscillator strength used to normalize the measured cross sections. Therefore, the discrepancy at near-zero momentum transfer could be addressed by renormalizing the measured DCSs. At higher momentum transfers, the agreement could be enhanced by improving the accuracy of the DCSs, as even a small difference in DCS significantly impacts the GOS.

4. Conclusion

We performed RDW calculations for electron impact excitation from the ground state $6p^3\ ^4S_{3/2}$ to the excited state $6p^27s\ ^4P_{1/2}$ of bismuth. The DCSs and ICSs were computed over an incident electron energy range of 10–100 eV and compared against the measured data from the previous studies. The calculated DCSs showed a satisfactory match with the measurements and followed the shape and features of experimental data, though there were some discrepancies at specific scattering angles. A complete inclusion of non-local exchange kernel and polarization potential during the continuum electron wavefunction generation may provide insight into the disagreement at the specific scattering angles. This remains open for further investigation. Similarly, the computed ICSs showed reasonable agreement with the measured cross sections with the underestimation for the 20 eV electron energy. The current study also analyzed the GOS derived from the calculated DCSs, highlighting their consistency with the reported data from Marinković *et al* [4], within the theoretical expectations. By far this work is the first theoretical study on the EIE of bismuth. It demonstrates the capability of computational implementation of the RDW approximation to predict the electron scattering properties in a reasonably accurate manner.

Acknowledgments

AKS acknowledges the Ministry of Education India for providing a PhD fellowship. The authors acknowledge National Supercomputing Mission (NSM) for providing computing resources of 'PARAM Ganga' at Indian Institute of Technology Roorkee, which is implemented by C-DAC and supported by the Ministry of Electronics and Information Technology (MeitY) and Department of Science and Technology (DST), Government of India.

Data availability statement

All data that support the findings of this study are included within the article (and any supplementary files).

ORCID iDs

Aloka Kumar Sahoo https://orcid.org/0000-0003-2441-4075
Lalita Sharma https://orcid.org/0000-0003-0316-0977

References

[1] Jacobs J M and Dworetsky M M 1982 *Nature* **299** 535–6
[2] Wahlgren G M, Brage T, Gilliland R L, Johansson S G, Leckrone D S, Lindler D J and Litzen U 1994 *apjl* **435** L67
[3] Predojević B, Pejčev V, Šević D and Marinković B P 2014 *J. Phys. Conf. Ser.* **565** 012019
[4] Marinković B P, Predojević B, Šević D and Pejčev V 2016 *J. Phys. B: At. Mol. Opt. Phys.* **49** 235203
[5] Williams W, Trajmar S and Bozinis D G 1975 *J. Phys. B: At. Mol. Phys.* **8** L96
[6] Joachain C J 1975 *Quantum Collision Theory* (North-Holland Pub. Co.)
[7] Balashov V V, Grum-Grzhimailo A N and Kabachnik N M 2000 *Polarization and Correlation Phenomena in Atomic Collisions* (Springer)
[8] Zuo T, McEachran R P and Stauffer A D 1991 *J. Phys. B: At. Mol. Opt. Phys.* **24** 2853
[9] Chauhan R K, Srivastava R and Stauffer A D 2005 *J. Phys. B: At. Mol. Opt. Phys.* **38** 2385
[10] Sharma L, Surzhykov A, Srivastava R and Fritzsche S 2011 *Phys. Rev.* A **83** 062701
[11] Froese Fischer C, Gaigalas G, Jönsson P and Bieroń J 2019 *Comput. Phys. Commun.* **237** 184–7
[12] Jönsson P *et al* 2023 *Atoms* **11** 68
[13] Zuo T 1991 *Ph.D thesis* York University, Toronto
[14] Roman V, Gomonai A I, Sharma L, Sahoo A K and Gomonai A N 2022 *J. Phys. B: At. Mol. Opt. Phys.* **55** 165203
[15] Gomonai A, Roman V, Gomonai A, Sahoo A K and Sharma L 2022 *Atoms* **10** 136
[16] Guo-xin C 1996 *Phys. Rev.* A **53** 3227–36
[17] Zhang H L and Sampson D H 1993 *Phys. Rev.* A **47** 208–14
[18] Parpia F A and Mohanty A K 1992 *Phys. Rev.* A **46** 3735–45
[19] Gaigalas G 2022 *Atoms* **10** 129
[20] Fritzsche S 2019 *Comput. Phys. Commun.* **240** 1–14
[21] Gaigalas G and Fritzsche S 2021 *Comput. Phys. Commun.* **267** 108086
[22] Gu M F 2008 *Can. J. Phys.* **86** 675–89
[23] Avdonina N B, Felfli Z and Msezane A Z 1997 *J. Phys. B: At. Mol. Opt. Phys.* **30** 2591
[24] Kramida A, Ralchenko Y, Reader J and NIST ASD Team 2023 Available: https://physics.nist.gov/asd [2024, May 17]. National Institute of Standards and Technology, Gaithersburg, MDNIST Atomic Spectra Database (ver. 5.11), [Online]
[25] George S, Munsee J H and Vergès J 1985 *J. Opt. Soc. Am.*B **2** 1258–63
[26] Caiyan L, Berzinsh U, Zerne R and Svanberg S 1995 *Phys. Rev.* A **52** 1936–41
[27] Lide D (ed) 2005 *CRC Handbook of Chemistry and Physics Internet Version 2005* (CRC Press)